VI International Conference on Computational Methods in Marine Engineering
MARINE 2015
F. Salvatore, R. Broglia and R. Muscari (Eds)

LONG-TERM GLOBAL RESPONSE ANALYSIS OF A VERTICAL AXIS WIND TURBINE SUPPORTED ON A SEMI-SUBMERSIBLE FLOATING PLATFORM: COMPARISON BETWEEN OPERATING AND NON-OPERATING WIND TURBINE LOAD CASES

MAURIZIO COLLU[*], LANCE MANUEL[†], MICHAEL BORG[+], JINSONG LIU[†]

[*] Offshore Renewable Energy Engineering Centre
Cranfield University
Cranfield, MK43 0AL, UK
e-mail: maurizio.collu@cranfield.ac.uk, www.cranfield.ac.uk

[†] Dept. of Civil, Architectural and Environmental Engineering
University of Texas at Austin
Austin, Texas, USA
email: lmanuel@mail.utexas.edu, jinsongliu@utexas.edu

[+] Department of Wind Energy
Technical University of Denmark
Roskilde, Denmark
email: borg@dtu.dk

Key words: Offshore wind, floating wind turbines, VAWT, dynamics, long-term response

Abstract. This study continues [1] the examination of the long-term global response of a floating vertical axis wind turbine (VAWT) situated off the Portuguese coast in the Atlantic Ocean. The VAWT, which consists of a 5-MW 3-bladed H-type rotor developed as part of the EU-FP7 H2OCEAN project, is assumed to be mounted on the OC4 semi-submersible floating platform. Adding a non-operational load case (wind speed ~35m/s), the sea states identified are used to carry out coupled dynamics simulations using the FloVAWT design tool, for which an improved wave elevation and relative force/moment time signals approach is adopted, as well as also taking into account the drag generated by the wind turbine tower. Short-term turbine load and platform motion statistics are established for individual sea states that are analysed. The long-term reliability yields estimates of 50-year loads and platform motions that takes into consideration response statistics from the simulations as well as the metocean (wind-wave) data and distributions. The results show that it is not necessarily the load cases associated with the highest wind speed that lead to the highest displacements and tensions in the mooring lines; differences among the highest values in some load cases are too similar to establish which one should be considered in a conceptual/preliminary design phase. Also, the aerodynamic drag model needs to be further developed to improve its accuracy. These results and insights contribute to the development of improved floating VAWT design guidelines for reducing the cost of offshore wind energy generation.

1 INTRODUCTION

The pursuit of reducing the cost of offshore wind energy in deep waters has led to a re-emerging interest in vertical-axis wind turbines (VAWTs) for floating applications due to potential advantages over conventional horizontal-axis wind turbines (HAWTs) [2], [3]. Previous research studies have focused on exploring the design space of floating VAWTs, such as the DeepWind concept [4] and the NOVA concept [5]; development of coupled dynamics numerical models, with most prominent developments outlined by [6][7][8]; and investigating the underlying dynamics and performance of floating VAWTs, with [9] assessing the global motion performance of the DeepWind concept and [10] investigating the frequency-domain characteristics of floating VAWT global aerodynamic loads.

The present work is a continuation of a recent work by the authors [1] on the estimation of the global dynamic response of a reference floating VAWT system. In the previous work, the characteristic or nominal wind turbine loads associated with long return periods on the order of 50 years, *in operational condition* (i.e. wind speed below the cut-out speed) have been considered. An alternative procedure to the classic one requiring sweeping the entire space of sea states for the turbine loads simulations has been adopted. Using the Environmental Contour (EC) method developed by [11], founded on structural reliability principles, it makes possible to evaluate only a subset of the sea states, which must be identified given metocean data and the target return period of interest. Essentially, 50-year loads can be approximately estimated using only the largest extreme load levels from among all the critical sea states first identified. For further details see [1]. It is important to highlight that the reason the method is approximate is that the reliability target that is the starting point for the analysis assumes a linearized "limit state" that defines the overall loads analysis. Additionally, the EC method can require some correction if load variability conditional on sea state definition is high.

In the present work the approach is extended toward the wind turbine *non-operational conditions*, i.e. for the extreme wind speeds above the cut-out speed, and a comparison between the global motion in these conditions and the global motion in the operational conditions will be made. From a design point of view this can be an important analysis to perform, since in principle the extreme non-operational conditions, characterised by higher wind speeds, may not be necessarily the ones driving the design.

1.1 Problem statement

To date the standard, guidelines and recommended practices developed for floating wind turbines have been focusing on HAWT [12]–[14]. As floating VAWT aerodynamic loads are significantly different to floating HAWT aerodynamic loads [15], understanding the influence of such loads on the long-term dynamic response to metocean conditions of floating VAWTs is crucial to better formulate future design standards/practices/guidelines. This study aims to compare the operational versus non-operational long-term dynamic response characteristics of the floating VAWT system presented, in order to derive an understanding on which conditions can be the most demanding ones and therefore can drive the design of the offshore floating wind turbine system.

2 FOWT SYSTEM DEFINITION

This case study considers the same systems analysed in [1], a floating VAWT semi-submersible system, conceptually depicted in Figure 1.

2.1 Wind turbine

The wind turbine consists of a 3-bladed H-type rotor developed during the FP7 H2OCEAN project [16] that has a power capacity of 5MW at an above the rated wind speed of 12m/s. The cut-in speed and cut-out speed are respectively 5m/s and 25m/s, with a rated rotational speed of 7.4rpm, a rotor radius of 58.6m, a blade length of 100m and chord length of 4.7m.

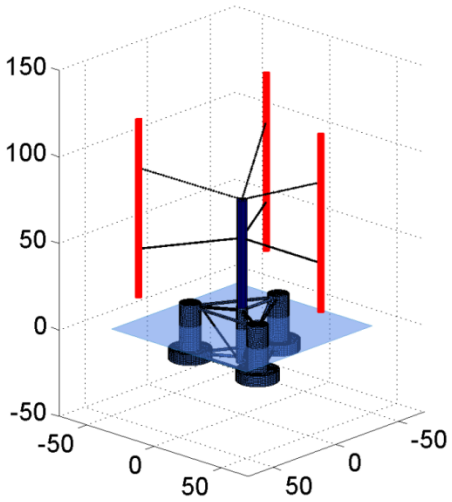

Figure 1: Visualisation of the floating VAWT considered

2.2 Floating support structure

The turbine is mounted on the OC4 semi-submersible system, originally developed by Robertson [17], also shown in Figure 1. As the turbine mass differs from the original payload of the OC4 semi-submersible, the ballast was adjusted to maintain the same draft whilst the same mooring system configuration was kept. The main characteristics of the floating system, *including* wind turbine inertia, are presented in Table 1.

Table 1: Platform main characteristics

Platform mass (tonnes)	14,108
Operating Draft (m)	20
Centre of gravity, from keel (m)	11.34
Hydrostatic restoring stiffness, heave (kN/m)	3.84E+06
Hydrostatic restoring stiffness, roll (kN-m/rad)	8.08E+06
Hydrostatic restoring stiffness, pitch (kN-m/rad)	8.08E+06

3 METHODOLOGY: LONG-TERM LOADS ASSESSMENT

3.1 Description of site and load cases

The site selected for this study is the Buoy Cabo Silleiro site in the Atlantic Ocean, off the

N-W coast of Spain, whose joint environmental data on wind speed, wave height, and wave period, obtained using a numerical hindcast model, have been provided in the study by Li et al. [18]. Joint probability distributions for this site (identified as Site No. 3 in [18]) for three random variables, U_w, the mean wind speed at 10 meters height, H_s, the significant wave height, and T_p, the wave spectral peak period are available. We assume Weibull distributions for U_w and for H_s given U_w and a lognormal distribution for T_p given U_w and H_s. The cumulative distribution functions for these variables are given as follows:

$$F_{U_w}(u) = 1 - \exp\left[-\left(\frac{u}{\beta}\right)^{\alpha}\right] \tag{1}$$

$$F_{H_s|U_w}(h|u) = 1 - \exp\left[-\left(\frac{h}{\beta_h(u)}\right)^{\alpha_h(u)}\right] \tag{2}$$

$$T_m(u,h) = \frac{\mu_T(u,h)}{\sqrt{1+\delta_T(h)^2}} \tag{3a}$$

$$\mu_T(u,h) = \bar{\mu}_T(h)\left[1 + \theta\left[\frac{u-\bar{u}(h)}{\bar{u}(h)}\right]^{\gamma}\right] \tag{3b}$$

Parameters appearing in Eqs. (1) to (3) that are needed to define the random variables are presented in Table 2 for the site selected.

Table 2. Environmental Random Variable Distribution Parameters

Parameters needed for random variables	
For U_w [Eq. (1)]	$\alpha = 2.002, \beta = 7.866$
For $H_s \mid U_w$ [Eq. (2)]	$\alpha_h(u) = 1.643 + 0.093u^{1.000}$ $\beta_h(u) = 1.969 + 0.031u^{1.644}$
For $T_m(u,h)$ [Eq. (3)]	$\bar{\mu}_T(h) = 5.0 + 5.970h^{0.223}$ $\bar{u}(h) = 1.0 + 4.055h^{0.466}$ $\delta_T(h) = 0.030 + 0.234h^{-0.221}$ $\theta = -0.143, \gamma = 1.0$

If we introduce two independent standard normal random variables, U_1 and U_2, then we can map the physical variables, U_w and H_s, to U_1 and U_2 as follows:

$$\Phi(u_1) = F_{U_w}(u) \tag{4}$$

$$\Phi(u_2) = F_{H_s|U_w}(h|u) \tag{5}$$

Note that we are not modelling the wave spectral period as fully random but will use its conditional median (for any U_w and H_s). These sea state parameters are used to define 6 of the load cases studied.

3.2 Inverse FORM or Environmental Contour (EC) method

If we employ the Inverse FORM or Environmental Contour (EC) method, we can derive 50-year return period values, y_{50}, for any response or load variable of interest, Y, as follows. First, because we are carrying out 1-hour simulations, we determine what the probability of

exceeding y_{50} in 1 hour—this is $1/(50\times365.25\times24) = 2.28\times10^{-6}$. In the EC method, we find the target reliability index, β, which is equal to $-\Phi^{-1}(2.28\times10\text{-}6)$, or 4.58. The 50-year contour that needs to be searched is that for which $U_1^2+U_2^2 = \beta^2$. The EC method, originally developed by Winterstein et al. [11] has been used in long-term reliability analyses for HAWTs by Agarwal and Manuel [19], Saranyasoontorn and Manuel [20], [21]; some refinements in those studies were also presented to directly account for response variability using 3-D Inverse FORM, which is a generalized version than the EC method. Using Eqs. (4) and (5), this contour can be constructed in physical space and allows us to define pairs of values (U_w, H_s) that need to be evaluated in 1-hour turbine response simulations. Using a power-law wind shear profile with an exponent of 0.1, the U_w values at 10-m elevation ae converted to hub-height wind speed values, U_{hub}, at 89 m. For any turbine response variable of interest, Y, the design 50-year return period is that value among all the (U_{hub}, H_s) pairs that leads the largest extreme 10-min value of Y. Representative sea states on the 50-year environmental contour that span the wind speed operating range of the turbine are presented in Table 3. Six of these load cases are defined per details provided in Table 2. The last load case (LC7) applies to the turbine is in a non-operating condition where the sea state is taken to be very severe and defined by the 50-year wind speed in combination with the 50-year significant wave height and associated wave period.

Table 3: Seven representative (U_w, H_S) pairs evaluated in the EC approach to obtain 50-y turbine load/response

Load case	U_{hub} (m/s)	RPM	H_s (m)	T_p (s)
LC1	8	4.96	8.26	14.16
LC2	11	6.82	8.68	13.92
LC3	14	5.30	9.23	13.71
LC4	17	5.20	9.84	13.53
LC5	20	5.20	10.48	13.36
LC6	23	5.20	11.09	13.19
LC7	35	0	12.53	13.11

3.3 Aero-hydro-mooring coupled model of dynamics simulations

The coupled dynamics numerical model utilised in this study is FloVAWT, as presented by Collu and Borg [8]. FloVAWT consists of a momentum-based aerodynamic model utilising a novel velocity formulation and a hydrodynamic model based on the Cummins equation with radiation-force state-space approximation and a global quadratic viscous drag model (coefficients of which were obtained from Coulling et al. [22]). A quasi-static catenary mooring line model was used to represent the mooring system and rigid body dynamics were considered for both the turbine and floating support structure. Lastly no detailed turbine control system was implemented; the rotational speed of the turbine was prescribed based on the mean wind speed for each simulation. For each pair of values (U_{hub}, H_s) defined above, ten time-domain realisations were simulated, each time utilising random seeds in the generation of the sea surface elevation process and the turbulent wind field using TurbSim [23]. We used a JONSWAP spectrum (peakedness factor, $\gamma = 3.3$) for the wave simulation of long-crested waves; for the wind simulations, we assumed IEC turbulence category C (reference turbulence intensity = 0.12) [24]. For all simulations, the global sampling rate for output data

was set to 10Hz.

Even if continuing and expanding the work presented by the authors in [10], two model improvements have been implemented.

The distributed drag forces on the tower due to the incident wind are obtained with the following equation:

$$\mathrm{dF}(z) = 0.5\rho A C_D dz U_R^2 \tag{5}$$

where z is the height of the distributed force on the tower, ρ is the air density, A is the cross-sectional area of the tower section, C_D is the section drag coefficient, dz is the discretization length and U_R is the relative fluid velocity, including platform-induced motions. During time domain simulations the tower is discretized into a number of nodes and at each time step the instantaneous positions of these nodes and instantaneous relative velocities experienced at these positions are calculated such that the above equation can be implemented to establish the distributed drag force which is then numerically integrated along the length of the tower. In this study, the drag coefficient was step to 1.0, and the free stream velocity was considered when calculating relative velocity contributions from incident wind.

As regard the generation of the surface elevation time signals for each load case, having as target the wave spectra presented in Table 4, and the evaluation of relative wave loads on the structure, a new approach has been implemented, based on the IFFT approach as presented by Jonkman [25]. The new approach has been applied also to the load cases already analysed in the previous work by the authors [10]. As it will be seen, the responses evaluated are different from the values in the previous work, and this can be justified analysing the force and moments RAOs functions, i.e. the transfer functions between the elevation of the wave and the forces/moments on the structure. In Figure 2 it can be seen that the approach used previously was not able to correctly derive the heave force RAO for frequencies above around 0.7 rad/s, while the new IFFT approach follows consistently the target curve (frequency domain model). In Figure 3 it illustrated how the old approach matches the target curve for frequencies above 0.9 rad/s, while the new IFFT approach shows to satisfy well the target frequency curve over the entire range of frequencies.

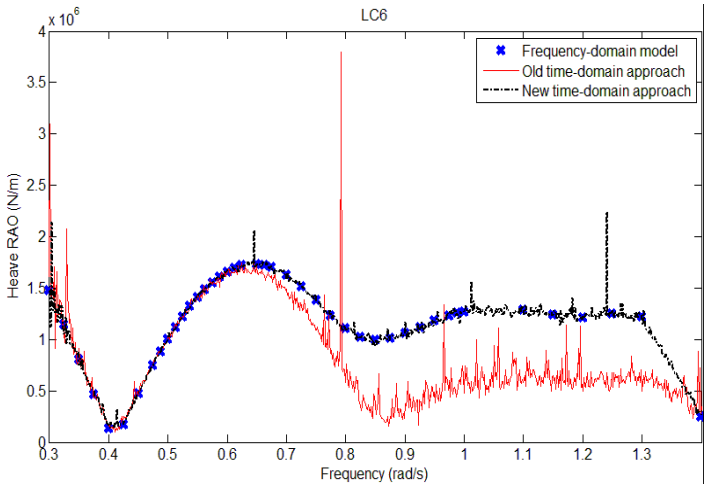

Figure 2: Heave Force RAO - LC6, target VS old approach VS new approach

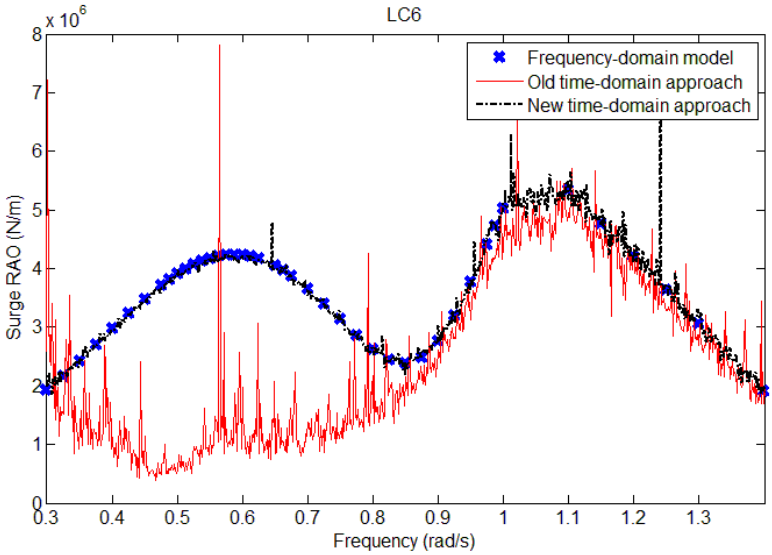

Figure 3: Pitch Moment RAO - LC6, target VS old approach VS new approach

In the time simulation, from a displacement point of view, there is a less than 2m difference as regard the linear displacement degrees of freedom between adopting the old time-domain approach and the new IFFT time-domain approach, while the rotational degrees of freedom 50-year responses are basically the same. As regard the differences in terms of mooring systems they are lower than 15% for the fairlead and anchor tensions, for both lines.

4 RESULTS AND DISCUSSION

In Figure 4 are represented the surge, sway, and heave 50-year responses of the FOWT system considered, from ~8m/s (LC1) to ~35m/s (LC7), with associated H_S and T_P (Table 2). Similarly, in Figure 5 are represented the 50-year responses in roll, pitch and yaw for LC1 to LC7. Figure 6 represents the 50-year mooring system tension responses, at the fairleads ('Fair' in the graph) and at the anchor ('Anch'), for lines 1 and 2. Lines 2 and 3 are placed symmetrically relative to the aligned wind and the long-crested waves, so they share the load, while Line 1 is the upwind line, and carries alone the loads on one side.

4.1 Surge, sway, and heave 50-year responses

First of all it can be seen that the highest displacements are in surge, and this is to be expected as the long-crested waves are aligned with the x-axis, as well as the wind direction.

As regard surge, the dominant scenario is LC6 with a 50-y response around 13.5m, but LC7 and LC5 are very close, with a response around 13.3m and 13m. The important observation is that even if LC7 represents a load case with a higher wind speed and a higher significant wave height (the peak period is similar to LC5 and LC6), it has to be considered that the wind turbine is operating for LC5 and LC6, while is not operating in LC7 conditions, and therefore the total aerodynamic forces acting on the wind turbine do not uniformly increase augmenting the wind speed: for LC1 to LC6, the aerodynamic forces acting on the blades are the dominant ones, while afterward the loads acting on the tower are the major contributors. No 2nd order wave loads have been included, so the net effect in surge can be

considered to be due only to aerodynamic forces.

Heave displacement is not substantially affected by the different loads in the different load cases, since both aerodynamic and hydrodynamic forces main components are not in this direction. For sway, the dominant load case is LC7, showing a clear peak in displacement for the relative wind and wave conditions.

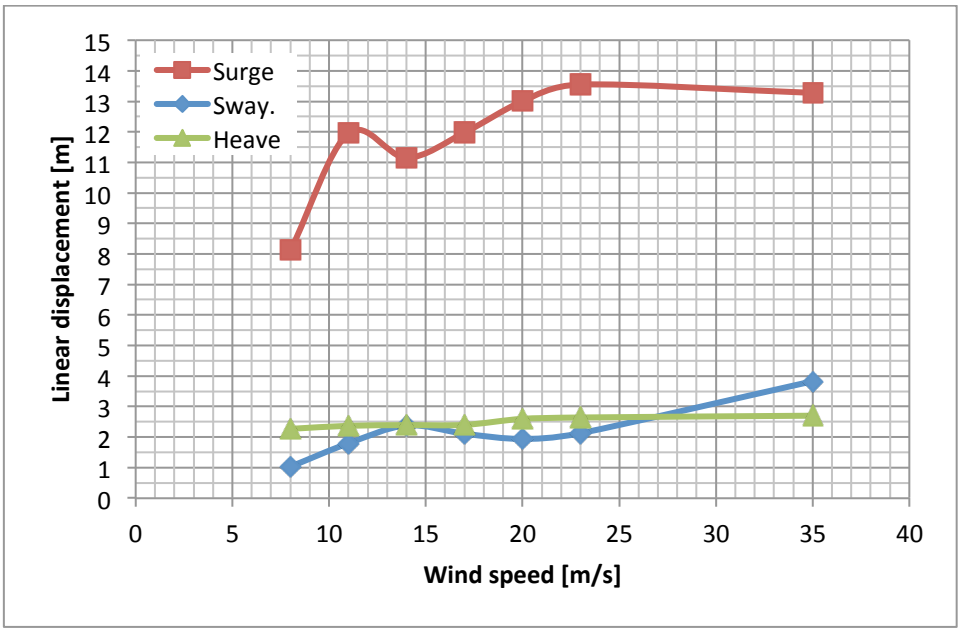

Figure 4: Surge, sway, and heave 50-year responses, for LC1 to LC7

4.2 Roll, pitch and yaw

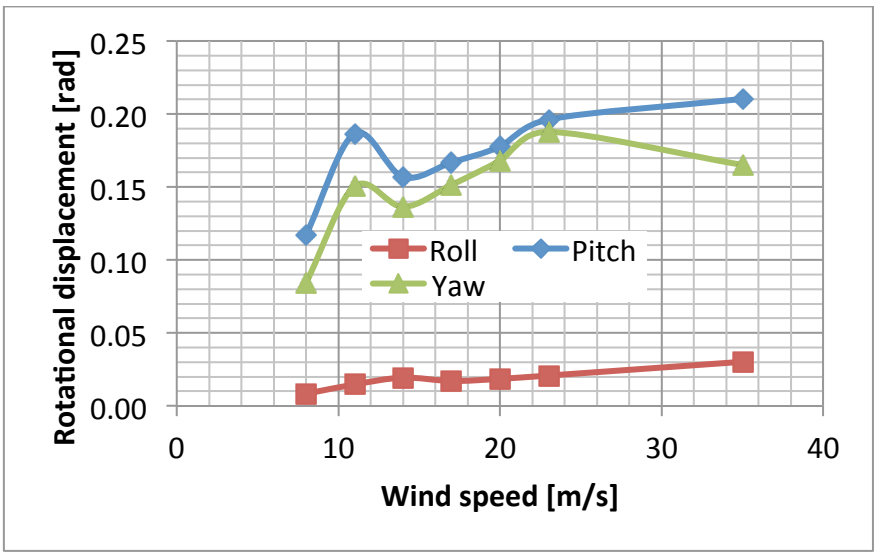

Figure 5: Roll, pitch, and yaw 50-year responses, for LC1 to LC7

Pitch and yaw are the rotational degrees of freedom that are most excited, and this is expected due to both the wind direction and the long-crested wave propagation direction aligned with the x-axis: while the wind turbine is operating (LC1 to LC6), the aerodynamic

thrust acting on the wind turbine, multiplied by the distance between the aerodynamic centre of pressure and the point where the thrust is reacted (mooring lines), imposes an inclining moment that leads to a pitch angle of inclination. At the same time, the aerodynamic torque is eventually reacted by the mooring system, leading to a yaw angle: being a VAWT, this moment is substantial. As regard the roll degree of freedom, again since the axis of rotation of the wind turbine is vertical, due to the gyroscopic effect, accelerations in the pitch degrees of freedom result in accelerations in the roll degree of freedom, but these are much smaller than the moments imposed in pitch by the wave loading, and therefore the roll rotational displacement is much smaller than the pitch one.

At LC7, the pitch angle increases while the yaw angle decreases. This is mainly due to the fact that at LC7 conditions the wind turbine is no longer operating (parked conditions), and therefore the yaw moment due to the aerodynamics is much less substantial, leading to a lower yaw angle. As regard the pitch angle, even if for LC7 the aerodynamic inclining moment is lower than the one for LC6, the LC7 H_S is ~1.5m higher, leading to a maximum inclining moment higher for this sea state.

As a general observation though, the difference between the 50-year pitch inclination angle in LC6 and LC7 is around 0.014rad, or ~0.8 deg. This difference is too little to be able to state that, as regard pitch rotational angle, LC7 is the dominant load case, and further investigations are needed. The approach adopted to derive the drag force on the tower (Eq. 5) is approximated and conservative, and therefore these results highlight the need to further refine the approaches used to evaluate the total aerodynamic forces on the turbine, in order to better determine the load cases driving the design of the FOWT.

4.3 Fairlead and anchor tensions on line 1 and line 2

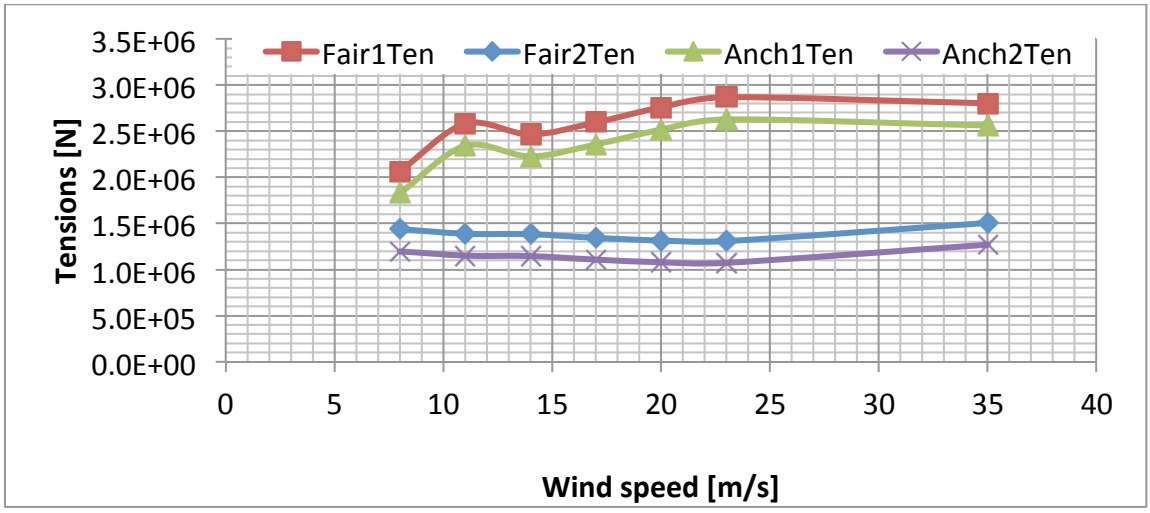

Figure 6: Fairlead and anchors tensions, 50-y responses, for LC1 to LC7

Fairlead and anchor tensions on line 1 are higher than those relative to line 2 as expected, since line 1 is the upwind line, aligned with the wind and the long-crested wave propagation directions. There are two symmetric lines downwind, line 2 and 3. The tensions in line 1, both at the fairlead and the anchor points, follow, as expected, the trend of the surge displacement curve: the peak is for LC6, but similar values are obtained for LC5 and LC6.

Nonetheless, as observed also for surge and pitch, the differences among the tensions in these three load cases are not substantial enough to state that one LC is definitely dominant with respect to the others, especially from a design point of view. As reported in Table 4, unless for fairlead 2 tensions, the difference between the highest and lowest tensions across LC5, 6, and 7 are equal to or lower than 4%. The quasi-static catenary mooring model adopted to estimate the tensions on the mooring lines has been validated with an error below 1%[8], therefore reinforcing the previous conclusions more effort should be put in the development of a more refined approach to estimate the aerodynamic forces on the tower, in order to establish with more accuracy which one is the load case driving the sizing (at a preliminary step) of the mooring system.

Table 4: Fairlead and anchor 50-year response tensions for line 1 and 2, value and differences with respect to LC5

Load Case	Fair1Ten	Delta	Fair2Ten	Delta	Anch1Ten	Delta	Anch2Ten	Delta
5	2.76E+06	\	1.32E+06	\	2.52E+06	\	1.08E+06	\
6	2.87E+06	4%	1.31E+06	0%	2.63E+06	4%	1.07E+06	-1%
7	2.80E+06	2%	1.51E+06	15%	2.56E+06	2%	1.27E+06	-3%

5 CONCLUSIONS

This paper has presented a methodology to estimate the global motion and mooring line tension long-term responses (50-year) for a conceptual floating VAWT case study, using an inverse FORM/Environmental contour methodology to establish the load cases to be considered and using the FloVAWT aero-hydro coupled model of dynamics as design tool.

Continuing and further developing the work presented previously by the authors [1], an additional non-operational load case has been added (LC7, wind speed ~35m/s), and all the load cases have been re-analysed with an improved approach to estimate the wave elevation and force/moments RAO time-signals and an improved tower drag estimation approach. The results obtained differ in some cases with respect to the previous analysis, due to the refined approach.

Two are the main conclusions that can be derived by the results. First of all, as also concluded in the previous work, the 50-year global platform motions and mooring line tensions are not necessarily driven only by the 50-year return metocean conditions characterised by the highest wind speeds, as the largest turbine thrust and associated loads occur at the maximum wind speed, different from that for variable-speed pitch-controlled HAWTs for which the maximum aerodynamic forces generally occur at the rated wind speed. Therefore, since the early phases of the design of a floating offshore VAWT system, it is important to consider a number of load conditions.

Secondly, the 50-year response values obtained for LC5, LC6 and LC7 are, in general, the

highest ones, but in some cases are not different enough to be able to determine which one is the dominant, design-driving loading condition. As mentioned, the model adopted to estimate the aerodynamic loads should be further refined, and in particular the conservative model adopted for to estimate the tower drag should be revised. Having a higher accuracy model will allow to determine with more precision which one is the load case that can be considered in the early stages of the design. Since the mooring line tension values are strictly linked to aerodynamic and hydrodynamic forces acting on the structure, the previous suggested improvement will benefit also these estimates.

The methodology and results presented herein provide useful insights into designing large floating VAWTs, identifying design issues due to the underlying dynamics of such systems.

REFERENCES

[1] M. Borg, L. Manuel, M. Collu, and J. Liu, "Long-term Global Performance Analysis of a Vertical-Axis Wind Turbine Supported on a Semi-Submsersible Floating Platform," in *Proceedings of the ASME 34th International Conference on Ocean, Offshore and Arctic Engineering (OMAE 2015)*, 2015.

[2] M. Borg, A. Shires, and M. Collu, "Offshore floating vertical axis wind turbines, dynamics modelling state of the art. part I: Aerodynamics," *Renew. Sustain. Energy Rev.*, vol. 39, pp. 1214–1225, Nov. 2014.

[3] A. Shires, M. Collu, and M. Borg, "FloVAWT: Progress on the development of a coupled model of dynamics for Floating offshore Vertical Axis Wind Turbines," in *The International Society of Offshore and Polar Engineers 2013*, 2013, no. 5.

[4] U. S. Paulsen, H. A. Madsen, K. A. Kragh, P. H. Nielsen, I. Barat, J. Hattel, E. Ritchie, K. Leban, H. G. Svendsen, and P. A. Berthelsen, "DeepWind - from idea to 5MW concept," *Energy Procedia*, vol. 53, pp. 23–33, 2014.

[5] A. Shires, "Design optimisation of an offshore vertical axis wind turbine," *Energy*, vol. 166, no. EN1, pp. 7–18, 2013.

[6] K. Wang, T. Moan, and M. O. L. Hansen, "A method for modeling of floating vertical axis wind turbine," in *Proceedings of the ASME 2013 32nd International Conference on Ocean, Offshore and Arctic Engineering*, 2013.

[7] H. Madsen, T. Larsen, L. Vita, and U. Paulsen, "Implementation of the Actuator Cylinder flow model in the HAWC2 code for aeroelastic simulations on Vertical Axis Wind Turbines," in *51st AIAA Aerospace Sciences Meeting including the New Horizons Forum and Aerospace Exposition*, 2013.

[8] M. Collu, M. Borg, A. Shires, F. N. Rizzo, and E. Lupi, "FloVAWT: Further Progresses on the Development of a Coupled Model of Dynamics for Floating Offshore VAWTs," in *ASME 2014 33rd International Conference on Ocean, Offshore and Arctic Engineering OMAE 2014*, 2014.

[9] L. Vita, "Offshore Floating Vertical Axis Wind Turbines with Rotating Platform," PhD Thesis, Riso DTU, 2011.

[10] Borg, "Offshore floating vertical axis wind turbines: development & applications of a coupled model of dynamics," Cranfield University, UK, 2014.

[11] S. Winterstein and T. Ude, “Environmental parameters for extreme response: Inverse FORM with omission factors,” Proceedings of ICOSSAR-93, Innsbruck, Austria, pp. 551–557, 1993
[12] DNV, “DNV-OS-J103 Design of Floating Wind Turbine Structures,” 2013.
[13] ABS, “Guide for building and classing floating offshore wind turbine installations,” 2013.
[14] BV, “Classification and Certification of Floating Offshore Wind Turbines,” Bureau Veritas, 2010.
[15] M. Borg and M. Collu, “A comparison between the dynamics of horizontal and vertical axis offshore floating wind turbines,” *Phil.Trans. Roy. Soc. A*, 2015.
[16] M. Collu, A. Shires, and M. Borg, “H2Ocean - D4 . 1 Report assessment on wind turbine types,” Cranfield, UK, 2014.
[17] A. Robertson, J. M. Jonkman, M. Masciola, H. Song, A. J. Goupee, A. J. Coulling, and C. Luan, “Definition of the Semisubmersible Floating System for Phase II of OC4.”
[18] L. Li, Z. Gao, and T. Moan, “Joint Environmental Data at Five European Offshore Sites for Design of Combined Wind and Wave Energy Devices,” in *Volume 8: Ocean Renewable Energy*, 2013, p. V008T09A006.
[19] P. Agarwal and L. Manuel, “Simulation of offshore wind turbine response for long-term extreme load prediction,” *Engineering Structures,* Vol. 31, No. 10, pp. 2236-2246, October 2009.
[20] K. Saranyasoontorn and L. Manuel, “Efficient models for wind turbine extreme loads using inverse reliability,” *Journal of Wind Engineering and Industrial Aerodynamics,* Vol. 92, No. 10, pp. 789-804, 2004.
[21] K. Saranyasoontorn and L. Manuel, “Design loads for wind turbines using the environmental contour method,” *Journal of Solar Energy Engineering,* Vol. 128, No. 4, pp. 554-561, 2006.
[22] A. J. Coulling, A. J. Goupee, A. N. Robertson, J. M. Jonkman, and H. J. Dagher, “Validation of a FAST semi-submersible floating wind turbine numerical model with DeepCwind test data,” *J. Renew. Sustain. Energy*, vol. 5, no. 2, 2013.
[23] D. Matha, J. M. Jonkman, T. Fischer, and M. Kuhn, “Model Development and Loads Analysis of a Wind Turbine on a Floating Offshore Tension Leg Platform,” in *European Offshore Wind Conference*, 2009, pp. 1–10.
[24] IEC, “IEC 61400-3, Wind Turbines – Part 3: Design Requirements for Offshore Wind Turbines,” 2007.
[25] J. M. Jonkman, “Dynamics of Offshore Floating Wind Turbines—Model Development and Verification,” *Wind EnergyWind Energy*, vol. 12, pp. 459–492, 2009.